

Resolution of interatomic distances in the study of local atomic structure distortions by energy-restricted x-ray absorption spectra

L. A. Bugaev, L. A. Avakyan, V. V. Srabionyan, and A. L. Bugaev

Physical Department, Southern Federal University, Zorge Street, 5, Rostov-on-Don 344090, Russia

(Received 29 April 2010; published 31 August 2010)

Applicability of the existing criteria for signal frequencies resolution to the problem of close interatomic distances determination by energy-restricted x-ray absorption spectra is studied within the approach based on the Fourier transformation and fitting procedures. Without losing generality, theoretical signals $\chi(k)$ of different k dependencies are used and among them—the signals $\chi(k)$ of x-ray absorption spectroscopy (k is the photoelectron's wave number). The last ones are calculated at different values of two interatomic distances R_1 and R_2 in a model of radial distribution of coordinating atoms in relation to the absorbing center, including the values of distances, which can't be resolved *a priori* according to the criteria. It is revealed that the boundary value of $\Delta R = |R_2 - R_1|$, at which the model of local structure distortions can be distinguished among other alternative ones by the used approach depends strongly upon the coincidence of the functional form of k dependence used for the fitting function with that of the studied signal $\chi(k)$, well known in x-ray absorption spectroscopy. In the case of coincidence, the boundary value of ΔR obtained by the restricted intervals $\Delta k \sim 3$ or 4 \AA^{-1} is approximately ten times smaller than that predicted by the existing criteria. The effect of statistical noise in spectrum intensity on the established ΔR value is analyzed.

DOI: [10.1103/PhysRevB.82.064204](https://doi.org/10.1103/PhysRevB.82.064204)

PACS number(s): 61.05.cj

I. INTRODUCTION

Atomic and electronic structures of materials at changing external conditions undergo various changes, resulted in phase transitions, reconstruction of the surface and changes in atoms valences. To determine the relation between performance and structures at these conditions, detailed information of their local atomic structure must be available, which can be obtained via new developed experimental techniques. One of the most effective techniques is provided by x-ray absorption spectroscopy (XAS), which is element specific and can be applied at extreme conditions. However, the spectra measured at these conditions are often restricted in energy: (i) for heterogeneous catalysts XAS measurements require time resolution, which limits the data range to the near edge (x-ray appearance near-edge structure) region;^{1,2} (ii) for materials under pressure the spectra are restricted due to the presence of Bragg reflections from the diamond anvils;³ (iii) at high temperatures the increased values of the Debye-Waller (DW) parameter diminish strongly the oscillations of the extended x-ray absorption fine structure (EXAFS) at large values of photoelectron wave numbers (k). For application of XAS to the study of materials' local structure by energy-restricted spectra several techniques for quantitative analysis are developed^{4–8} which often give the accuracy of the determined structural parameters for atom's coordination in amorphous or poorly ordered structures not worse than that provided by EXAFS. In the approach of,⁸ the Fourier transformation (FT) of spectrum is performed and the difficulties of structural analysis by the fitting procedure with limited number of varied parameters are overcome using the values of nonstructural parameters, established by appropriate reference compounds.⁹ The application of the approach to these compounds in Refs. 9 and 10 revealed that interatomic distances between the absorbing and the first neighboring atoms are determined with uncertainty of $\sim 0.01 \text{ \AA}$ by energy-restricted spectra.

In spite of the obtained results, the application of these techniques is restrained since the local-structure distortions are often characterized by the difference in interatomic distances $\Delta R \sim 0.1 \text{ \AA}$ in radial distribution of coordinating atoms around the absorbing one, which is less than the boundary values for distances resolution, estimated by the widely used criterion.¹¹ In the present paper the eligibility of application of this criterion to XAS, particularly within the approach based on FT and fitting procedures for structural parameters determination, is studied (Sec. II), using the calculated signals with various functional forms of k dependence and at different values of ΔR , including the ones, which can't be resolved *a priori* according to the analyzed criterion. The performed analysis gives the boundary values of ΔR in the model of distortions for coordinating atoms polyhedron, at which this model can be distinguished among others. The effect of statistical noise in intensity of spectrum on the established boundary values of ΔR is studied in Sec. III.

II. CRITERIA FOR INTERATOMIC DISTANCES RESOLUTION AND THEIR APPLICABILITY TO X-RAY ABSORPTION SPECTROSCOPY

In accordance with the signals theory¹² a certain function of time $f(t)$, which exists in the finite interval $[0, \tau]$ [so that $f(t) = 0$ for $t < 0, t > \tau$] and has a restricted frequencies spectrum with a maximum frequency ω_{\max} , is completely defined by limited set of independent parameters. The number of these parameters (or the degree of freedom N_{idp}) is determined by expression

$$N_{\text{idp}} = \frac{\omega_{\max} \cdot \tau}{\pi} + 1. \quad (1)$$

This result follows from the expansion of $f(t)$ in Fourier series and at the same time is a consequence of the sampling

method applied to $f(t)$. In this method the function is represented as a sampled one $f(t_m)$, defined in the sampling points t_m , $m=1, 2, 3, \dots, N_{\text{idp}}$. The sampling step δt in the t scale $\delta t = \tau/N_{\text{idp}}$ corresponds to the Nyquist frequency¹³ and the frequency resolution $\delta\omega$ in the conjugate ω scale, which characterizes the number of the distinguished frequencies in the $f(\omega)$ spectrum is given by

$$\delta\omega = \omega_{\text{max}}/N_{\text{idp}}. \quad (2)$$

To apply this result to x-ray absorption spectroscopy, the conjugate variables t and ω should be replaced with k and $2R$, respectively, as: $\tau \rightarrow \Delta k = (k_{\text{max}} - k_{\text{min}})$ —the extension of XAS signal in the scale of photoelectron wave numbers and $\omega \rightarrow 2R$ —the frequency in the conjugate scale of interatomic distances. As a result, Eq. (1) can be rewritten as¹⁴

$$N_{\text{idp}} = \frac{2R_{\text{max}}\Delta k}{\pi} + 1. \quad (3)$$

In last expression it is possible to extract the resolution δR of interatomic distances, defined according to Eq. (2) as $\delta R = R_{\text{max}}/N_{\text{idp}}$ and obtain

$$\delta R = \frac{\pi}{2\Delta k} \left(1 - \frac{1}{N_{\text{idp}}} \right). \quad (4)$$

For EXAFS analysis the extension of signal $\chi(k)$ —the normalized EXAFS function¹⁵ in the k scale is $\Delta k \sim 10\text{--}15 \text{ \AA}^{-1}$. For such an extended $\chi(k)$ signal, Eq. (3) gives $N_{\text{idp}} \sim 10$, so the second term in Eq. (4) is negligible and therefore

$$\delta R = \pi/(2\Delta k). \quad (5)$$

The last expression establishes the estimating criterion for interatomic distances resolution which is used in the EXAFS data analysis. According to it, two distances R_1 and R_2 from the absorbing center to the neighboring atoms, can not be resolved by the FT analysis of $\chi(k)$ over the available Δk interval if their difference is smaller then δR , i.e., if

$$\Delta R < \delta R = \pi/(2\Delta k).$$

The estimation by Eq. (5) gives the resolution limit of $\sim 0.15 \text{ \AA}$ for $\Delta k \sim 10 \text{ \AA}^{-1}$ in EXAFS analysis. However, if the restricted k intervals ($\Delta k \sim 3$ or 4 \AA^{-1}) are used then Eq. (3) gives $N_{\text{idp}} \sim 4$ and estimation of the limit for distances resolution must be performed by Eq. (4), which gives the value of $\delta R \sim 0.4 \text{ \AA}$. As was mentioned above, the presented values of limits for R resolution, provided by Eqs. (4) and (5), restrain the application of XAS to the analysis of local atomic-structure distortions, often characterized by the smaller values of $\Delta R \sim 0.1 \text{ \AA}$.

It must be emphasized, however, that the used expressions (4) and (5) are obtained under the general formulations of the sampling method and the Fourier analysis, applied to the arbitrary shape signals while in x-ray absorption spectroscopy the functional form of k dependence of $\chi(k)$ is well known.¹⁵ Besides, the mentioned above boundary conditions for the signals, used to derive Eqs. (4) and (5), are weakly suitable for the studied XAS signals and as was marked in¹⁶ “the definition of N_{idp} can provide only a rough estimate of

this number” (mainly because of the uncertainties in the choice of ω_{max} or $2R_{\text{max}}$ —authors comment). To avoid the use of the criteria based on N_{idp} notion, statistical procedures for nonlinear fitting were adopted for error evaluation problem in the structural analysis performed by EXAFS.¹⁶

The aim of this work is to establish the eligibility of application of the expressions (4) and (5) for resolution of close interatomic distances in the structural analysis performed by energy restricted XAS and especially in the determination of local structure distortions, often performed by the approach.^{9,17} In this approach the structural distortions around the absorbing atom are studied by the FT of experimental spectrum and the following fit of its Fourier image $[F(R)]$, performed by alternative models for radial distribution of coordinating atoms in relation to the absorbing one. Within the fit, the widths and the asymmetry of the coordinating atoms Fourier peak for the studied $\chi(k)$ and for the $\chi(k)$ of each model are compared in the same Δk intervals. The choice of an adequate model is made by the obtained values of the reduced square residual function, denoted as χ_v^2 and defined by the expression¹⁸

$$\chi_v^2 = \frac{N_{\text{idp}}}{N\nu\xi^2} \sum_{i=1}^N \{ \{ \text{Re}[F_{\text{data}}(R_i) - F_{\text{model}}(R_i)] \}^2 + \{ \text{Im}[F_{\text{data}}(R_i) - F_{\text{model}}(R_i)] \}^2 \} \quad (6)$$

where N is the total number of signal's points; $\nu = N_{\text{idp}} - N_{\text{varys}}$ is the number of degrees of freedom in the fit with the number of variables N_{varys} ; ξ is the single value of the uncertainty in the measurement. The values of χ_v^2 characterize the goodness of the fits and are used for comparison of fits with different number of variables.¹⁸ Moreover, the choice of the model is made by the values of DW parameter (σ^2), which characterizes both the atomic thermal motion and the degree of account of structural distortions by the used fit model.¹⁷

We apply this approach to theoretical functions $\chi(k)$ with various functional forms of k dependence. Each $\chi(k)$ is calculated either by its analytical expression, using different values of signal's parameters, or by FEFF8 code¹⁹—for XAS-like signals. In the last case, different numbers and values of interatomic distances R_i ($i=1, 2, \dots$ —depending upon the studied model of structural distortion) are used. Without losing generality, these $\chi(k)$ are considered then as the unknown signals for our analysis of applicability of the expressions (4) and (5) in XAS study.

A. Signals $\chi(k)$ with k dependence, differed from that of the fitting function

In x-ray absorption spectroscopy the approach is used, based on the account of photoelectron scattering paths in the vicinity of the absorbing atom.^{20,21} In this approach the function $\chi(k)$, which contains information of atom's local structure, is represented as a sum of terms

$$\chi(k) = \sum_{i=1}^{i_{\max}} \chi_i(k), \quad (7)$$

where i_{\max} is the total number of considered scattering paths, $\chi_i(k)$ is the contribution of i th scattering path. For the single scattering path (absorbing atom— i th neighboring atom) this term is determined by the expression¹⁵

$$\chi_i(k) = N_i S_0^2 \frac{|f_i(\pi, k)|}{k R_i^2} \sin[2k R_i + \arg f_i(\pi, k) + 2\delta_i] \times \exp(-2\sigma_i^2 k^2) \exp\left[-\frac{2R_i}{\Lambda(k)}\right] \quad (8)$$

In Eq. (8) N_i is the number of identical i th paths, $f_i(\pi, k)$ is the backscattering amplitude for i th neighboring atom, σ_i^2

is the DW parameter for i th path, S_0^2 is the reduction factor used to account for intrinsic losses, $\Lambda(k)$ is the mean-free path of photoelectron, $l=1$ for K absorption. This approach, with an accuracy of the use of a complex momentum for photoelectron scattering, is realized for generation of fitting function $\chi(k)$ in FEFIT code.²² The fit with $i_{\max}=1$ is often named as a single-shell fit, $i_{\max}=2$ —two-shells fit, etc.

To differ from the k dependence of the fitting function [Eq. (8)] of FEFIT, the first signal $\chi(k)$ to be studied was generated as a sum of two terms

$$\chi(k) = \{\chi_1(k) + \chi_2(k)\} \exp(-2\sigma^2 k^2), \quad (9)$$

where each of the two functions $\chi_i(k)$ ($i=1, 2$) is periodical, with a period $2\pi/R_i$ and is determined as

$$\chi_i(k) = \begin{cases} N_i \cdot \frac{2R_i}{\pi} \left(k - n \frac{2\pi}{R_i}\right), & -\frac{\pi}{2R_i} + n \frac{2\pi}{R_i} < k < \frac{\pi}{2R_i} + n \frac{2\pi}{R_i} \\ N_i \cdot \left[2 - \frac{2R_i}{\pi} \left(k - n \frac{2\pi}{R_i}\right)\right], & \frac{\pi}{2R_i} + n \frac{2\pi}{R_i} < k < \frac{3\pi}{2R_i} + n \frac{2\pi}{R_i} \end{cases} \quad (10)$$

$n=0, 1, 2, \dots$. Calculations of the total $\chi(k)$ were performed by Eqs. (9) and (10) with $\sigma^2=0.005 \text{ \AA}^2$, for $N_1=3, N_2=1$ [named in the following as (3+1) model], using $R_1=2.0 \text{ \AA}$ for χ_1 and for χ_2 the value of R_2 was changed from 2.0 \AA to 2.7 \AA , to get the resulting $\chi(k)$ for different values of $\Delta R = |R_2 - R_1|$ from 0 to 0.7 \AA .

The theoretical functions $\chi(k)$, calculated for these values of ΔR , were considered then as the unknown signals, and FT over two different k intervals $\Delta k=10 \text{ \AA}^{-1}$ and $\Delta k=3 \text{ \AA}^{-1}$ was applied to them. Each of the obtained $F(R)$ was fitted by FEFIT using an alternative fit models of $\chi(k)$: (3+1), (2+2), (2+3), (1+2+1), etc. The form of the fitting function, which realizes each model is determined by Eq. (7) with the number i_{\max} of terms $\chi_i(k)$ given by this model [for example, $i_{\max}=2$ for (2+3) model, $i_{\max}=3$ for (1+2+1) model, etc]. Each fitting term $\chi_i(k)$ in Eq. (7) is determined by Eq. (8), using $\lambda(k)=\infty$, $S_0^2=1$ and $\delta_i=0$ in the sine argument. For artificial signals of this and next sections, the values $|f_i(\pi, k)|=\text{const}$ and $\arg f_i(\pi, k)=0$ were used so as to perform fit everywhere through the work by the same code FEFIT. However, these particular values don't bring the lost of generality in the analysis of expressions (4) and (5) eligibility. The knowledge of the concrete function $f(\pi, k)$ becomes important in x-ray absorption spectroscopy, for real atomic systems to obtain high accuracy of structural parameters determination. Therefore, the effect of possible inaccuracies in $f_{A-B}(\pi, k)$ values (A —absorbing, B —neighboring atoms), due to uncertainties in preliminary knowledge of distance R_{A-B} used for $f_{A-B}(\pi, k)$ calculation, on the obtained resolution limits is discussed in Sec. II B considering As K -edge XAFS in indium arsenide.

For each model the fitted variables were R_i ($i=1, 2, \dots$ —depending upon the model) and σ^2 (the same for all χ_i). As an example, in Figs. 1(a) and 1(b) the function $\chi_1(k)$ and the total signal $\chi(k)$, calculated for $\Delta R=0.2 \text{ \AA}$, are presented. In Figs. 1(c) and 1(d) $F(R)$ of $\chi(k)$, obtained for $\Delta k=10 \text{ \AA}^{-1}$ and $\Delta k=3 \text{ \AA}^{-1}$, are compared with the results of their fit by the “true” (3+1) model [here and in the fol-

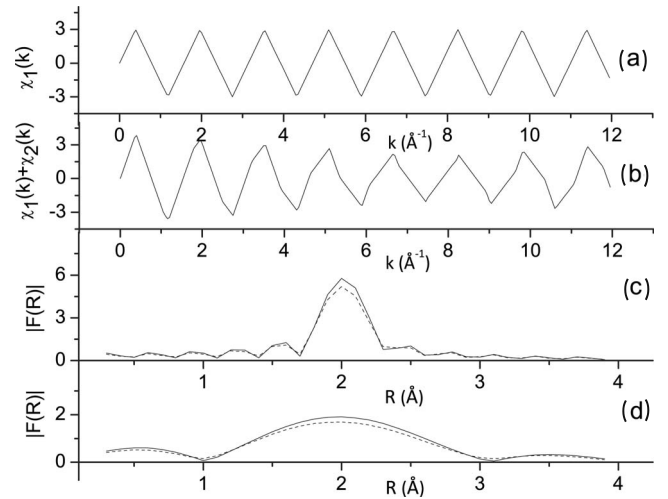


FIG. 1. $\chi_1(k)$ calculated by Eq. (10) with $R_1=2.0 \text{ \AA}$ —(a); the total signal $\chi(k)$, calculated by Eqs. (9) and (10) for (3+1) model with $\Delta R=0.2 \text{ \AA}$ —(b); $|F(R)|$ —the results of FT of $\chi(k)$, obtained for $\Delta k=10 \text{ \AA}^{-1}$ —solid curve in (c) and for $\Delta k=3 \text{ \AA}^{-1}$ —solid curve in (d), are compared with the results of corresponding fits by (3+1) model—dotted curves in (c) and (d).

lowing, the designation true is applied to the model, which was used for initial generation of the studied signal $\chi(k)$.

The goodness of the fits, performed by some of the considered models, is compared in Fig. 2(a) for FT of $\chi(k)$ over $\Delta k=10 \text{ \AA}^{-1}$ and in Fig. 2(b)—over $\Delta k=3 \text{ \AA}^{-1}$. The comparison shows that if the extended $\Delta k=10 \text{ \AA}^{-1}$ is used then the true (3+1) model is restored among other models beginning from $\Delta R=0.1 \text{ \AA}$ and gives the correct values of its parameters $R_1=2.0$, $R_2=2.13 \text{ \AA}$, and $\sigma^2=0.005 \text{ \AA}^2$. However, if the short k interval $\Delta k=3 \text{ \AA}^{-1}$ is used then the true (3+1) model is distinguished among others beginning from $\Delta R=0.5 \text{ \AA}$ and gives the correct values of its parameters $R_1=2.0 \text{ \AA}$, $R_2=2.5 \text{ \AA}$, and $\sigma^2=0.005 \text{ \AA}^2$.

As can be seen, the true model of the studied signal $\chi(k)$ is distinguished among others by the used approach beginning from the boundary values of ΔR , which are in good agreement with those, estimated by expressions (4) and (5).

These results are completely confirmed by the same FT analysis over $\Delta k=10 \text{ \AA}^{-1}$ and $\Delta k=3 \text{ \AA}^{-1}$ of the signal $\chi(k)$ generated by Eq. (9) as a sum of two terms $\chi_i(k)$ ($i=1,2$), determined as a periodic consequences of semicircles

$$\chi_i(k) = \begin{cases} N_i \cdot \sqrt{\left(\frac{\pi}{2R_i}\right)^2 - \left(k - \frac{\pi}{2R_i} - n\frac{2\pi}{R_i}\right)^2}, & n\frac{2\pi}{R_i} < k < \frac{\pi}{R_i} + n\frac{2\pi}{R_i} \\ -N_i \cdot \sqrt{\left(\frac{\pi}{2R_i}\right)^2 - \left(k + \frac{\pi}{2R_i} - n\frac{2\pi}{R_i}\right)^2}, & -\frac{\pi}{R_i} + n\frac{2\pi}{R_i} < k < n\frac{2\pi}{R_i} \end{cases} \quad (11)$$

$n=0,1,2,\dots$. This k dependence differs also from that of the fitting function [Eq. (8)] used in FEFIT. In Figs. 3(a) and 3(b) the term $\chi_1(k)$ calculated by Eq. (11) for $N_1=3$, $R_1=2.0 \text{ \AA}$ and the total signal $\chi(k)$ for $N_1=3$, $N_2=1$, $\Delta R=0.2 \text{ \AA}$, are presented. In Figs. 3(c) and 3(d) $F(R)$ of $\chi(k)$, obtained by $\Delta k=10 \text{ \AA}^{-1}$ and $\Delta k=3 \text{ \AA}^{-1}$, are compared with the fitting curves, obtained by the true (3+1) model. The results of the FT analysis, performed by different fitting models (3+1), (2+2), (2+3), (1+2+1), etc, are similar to those presented in Fig. 2 and show that the restoring of the true (3+1) model, used in the direct calculation of $\chi(k)$, is again obtained by the used approach of FEFIT beginning from the same values of ΔR , as are predicted by the expressions (4) and (5).

B. Signals $\chi(k)$ with the k dependence close to that of the fitting function

In this section, the signals $\chi(k)$ are considered, which have the functional forms of k dependence sufficiently close to the fitting function [Eq. (8)] of FEFIT, and contain two parameters R_1 and R_2 of different values, including the ones, not distinguished according to Eqs. (4) and (5).

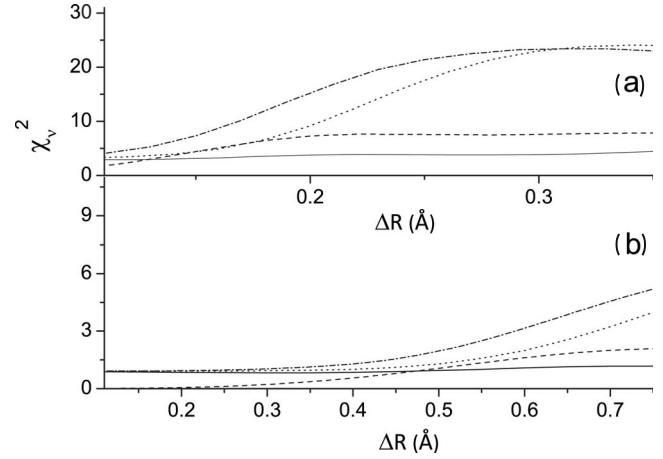


FIG. 2. The goodness of the fits (χ_v^2), obtained by different fitting models for $\chi(k)$, as a function of $\Delta R=|R_2-R_1|$ value used in the direct calculations of $\chi(k)$ by Eqs. (9) and (10) with $\sigma^2=0.005 \text{ \AA}^2$. Solid curve—fit by (3+1) or the true model; dotted curve—(2+2); dashed-dotted curve—(1+3); dashed curve—single term fit.

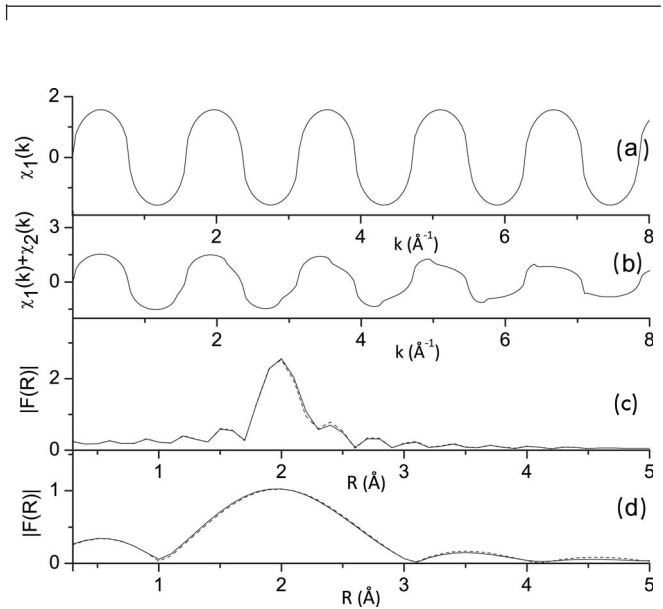
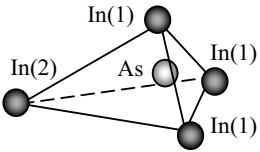
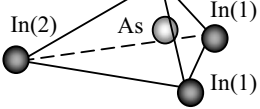
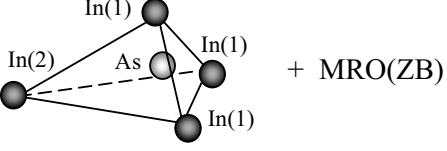
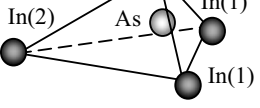
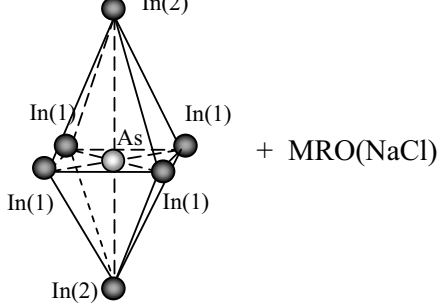
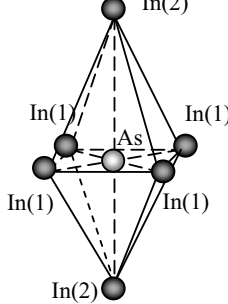
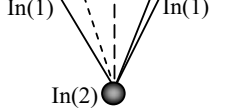


FIG. 3. $\chi_1(k)$ calculated by Eq. (11) with $R_1=2.0 \text{ \AA}$ —(a); the total signal $\chi(k)$, calculated by Eqs. (9) and (11) for (3+1) model with $\Delta R=0.2 \text{ \AA}$ —(b); $|F(R)|$ —the results of FT of $\chi(k)$, obtained for $\Delta k=10 \text{ \AA}^{-1}$ —solid curve in (c) and for $\Delta k=3 \text{ \AA}^{-1}$ —solid curve in (d), are compared with the results of corresponding fits by (3+1) model—dotted curves in (c) and (d).

TABLE I. Models and structural parameters for distorted As coordination in InAs, characterized by $\Delta R=0.03 \text{ \AA}$, used for FEFF8 simulations of $\chi(k)$ at $\sigma^2=0.007 \text{ \AA}^2$, in comparison with the results of FT-analysis of these $\chi(k)$ functions, performed over $\Delta k=4 \text{ \AA}^{-1}$, using alternative models of As coordination by In atoms.

Models for As local structure distortions in InAs used for FEFF8 simulations of $\chi(k)$ at $\sigma^2 = 0.007 \text{ \AA}^2$	Structural parameters and fit goodness (χ_v^2) obtained by FT of $\chi(k)$ over $\Delta k \sim 4 \text{ \AA}^{-1}$ and fit of $F(R)$, performed by the different models for As coordination			
	Fit models	$R_{\text{As-In}}$, (\AA)	σ^2 , (\AA^2)	χ_v^2
 <p style="text-align: center;">○ – As, ● – In</p>	4	2.62	0.008	0.35
	3+1	2.61, 2.65	0.007	0.21
$R_{\text{As-In}(1)} = 2.61 \text{ \AA}$, $R_{\text{As-In}(2)} = 2.64 \text{ \AA}$	2+2	2.59, 2.65	0.003	0.30
 <p style="text-align: center;">+ MRO(ZB)</p>	4	2.62	0.009	3.5
	3+1	2.61, 2.65	0.007	3.3
$R_{\text{As-In}(1)} = 2.61 \text{ \AA}$, $R_{\text{As-In}(2)} = 2.64 \text{ \AA}$	2+2	2.60, 2.65	0.008	3.6
 <p style="text-align: center;">+ MRO(NaCl)</p>	6	2.74	0.008	3.7
	4+2	2.73, 2.76	0.006	3.4
	3+3	2.72, 2.74	0.006	3.6
$R_{\text{As-In}(1)} = 2.73 \text{ \AA}$, $R_{\text{As-In}(2)} = 2.76 \text{ \AA}$	5+1	2.73, 2.80	0.002	3.7

The first of the studied signals is of the simplest model, determined by the expression (9) with $\chi_i(k) = N_i \sin(2kR_i)$, ($i=1,2$). Calculations of $\chi(k)$ were performed at the fixed values of $N_1=4$, $N_2=2$, named as (4+2) model with $R_1=2.0 \text{ \AA}$ and R_2 changed from 2.0 to 2.7 \AA , to get the resulting $\chi(k)$ at the values of ΔR from 0 to 0.7 \AA . The factor $\exp(-2\sigma^2 k^2)$ is included to make the expression for $\chi(k)$ closer to Eq. (8). The value of parameter $\sigma^2=0.005 \text{ \AA}^2$ was used.

Considering this theoretical $\chi(k)$ at each of the above values of ΔR as the unknown signals to be studied, the FT was applied to them over the two intervals $\Delta k=10 \text{ \AA}^{-1}$ and $\Delta k=3 \text{ \AA}^{-1}$. The obtained $F(R)$ were fitted by the same FEFFIT approach as in Sec. II A, using an alternative models for $\chi(k)$: (3+3), (4+2), (5+1), (2+2+2), (3+2), etc. The varied parameters were R_i ($i=1,2,\dots$ —depending upon the model)

and common σ^2 . For the single-term fit, N , R , σ^2 were varied. The goodness of the fits as a function of ΔR , obtained by some of these models, is compared in Fig. 4. As can be seen, the true model (4+2) for $\chi(k)$ becomes preferable among others beginning from the value of $\Delta R \sim 0.03 \text{ \AA}$ for $\Delta k=3 \text{ \AA}^{-1}$ and beginning from $\Delta R \sim 0.015 \text{ \AA}$ for $\Delta k=10 \text{ \AA}^{-1}$. Beginning from these ΔR values the true model gives also the correct values of parameters R_1 , R_2 , and σ^2 used in the initial calculations of $\chi(k)$. It should be noted that these boundary values of ΔR are of approximately ten times smaller than the limits established by Eqs. (4) and (5) for the studied signal.

To examine the signals of x-ray absorption spectroscopy, Fourier analysis was applied to theoretical $\chi(k)$, calculated for different models of As local structure distortions in indium arsenide (InAs), which occur at high pressures.²³ The

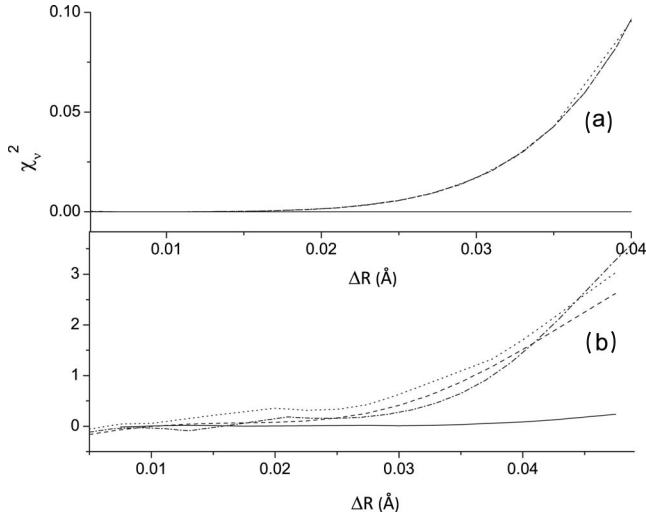


FIG. 4. The goodness of the fits (χ_p^2), obtained by different fitting models for $\chi(k)$, as a function of $\Delta R = |R_2 - R_1|$ value used in the direct calculations of $\chi(k)$ by Eq. (9) with $\chi_1(k) = 4 \sin(2kR_1)$, $\chi_2(k) = 2 \sin(2kR_2)$, $\sigma^2 = 0.005 \text{ \AA}^2$. Solid curve—(4+2) or true model; dotted curve—(3+3); dashed-dotted curve—(2+4); dashed curve—single term fit.

basis for these calculations is provided by the agreement of theoretical As K -edge absorption spectrum,²⁴ calculated by FEFF8, with the experimental spectrum of InAs at 0.4 GPa, which can be used as a reference compound for structural analysis of InAs at high pressures. In the first column of Table I the following models of As local structure are presented: (i) isolated distorted In tetrahedron; (ii) distorted In tetrahedron surrounded by the middle-range order (MRO) of zinc-blend structure; (iii) distorted In octahedron surrounded by the MRO of rocksalt structure (NaCl). The distortions of coordinating polyhedrons were made so as to get the above obtained boundary value of $\Delta R = 0.03 \text{ \AA}$ in radial distribution of As-In distances. The value of parameter $\sigma^2 = 0.007 \text{ \AA}^2$, typical for metals at room temperature,²⁵ was used in $\chi(k)$ calculations. These theoretical $\chi(k)$ were considered as the unknown signals for study, Fourier transformed over $\Delta k = 4.0 \text{ \AA}^{-1}$ and the results of the fit of corresponding $F(R)$, performed by some of the alternative models of As coordination are presented in Table I. The photoelectron backscattering amplitudes $f_{\text{As-In}}(\pi, k)$ used in the FT analysis were calculated at As-In distance $R_{\text{As-In}} = 2.7 \text{ \AA}$ —the averaged value over the most plausible As coordinations. Performed testing of the stability of the results of Table I upon the possible inaccuracies in $f_{\text{As-In}}(\pi, k)$ determination revealed that this amplitude is suitable for the structural analysis of samples with As-In bonds distributed from ~ 2.5 to 2.9 \AA .

As can be seen from the Table I, the true model of As local-structure distortion, characterized by $\Delta R = 0.03 \text{ \AA}$ in radial distribution of In atoms around the absorbing As, is preferable among other models within the used approach and gives the correct values of distances $R_{\text{As-In}(1)}$, $R_{\text{As-In}(2)}$, and σ^2 .

III. EFFECT OF STATISTICAL NOISE IN THE ANALYSIS OF ENERGY RESTRICTED X-RAY ABSORPTION SPECTRA

The effect of statistical noise in experimental x-ray absorption spectrum on the values of structural parameters determined by the extended Δk ranges of EXAFS data was studied in.^{26,27} In this section an analysis quite similar to Ref. 26 is performed for the energy-restricted x-ray absorption spectra with k ranges of ~ 3 or 4 \AA^{-1} . The aim is to reveal the effect of statistical noise on the boundary values of ΔR in the true model of radial distribution of atoms around the absorbing one, at which this model can be distinguished among other alternative models of local structure distortions by the used approach. For this purpose the intensity under statistical noise $I^{\text{st.n.}}$ was simulated via calculations using the expression: $I^{\text{st.n.}}(E_j) = I(E_j)(1 + \varepsilon_j)$, where E_j is the j th energy point in spectrum, $I(E_j)$ —the intensity calculated without the noise, ε_j —is the value of the statistical noise in j th point. Assuming that the noise in the incident intensity I_0 is negligible, compared to that for transmitted intensity I , the account of statistical noise in the calculations of $\chi(k)$ can be done by the expression

$$\chi^{\text{st.n.}}(k_j) = \chi(k_j) + \ln[1/(1 + \varepsilon_j)]. \quad (12)$$

Calculations of $\chi^{\text{st.n.}}(k_j)$ in each point k_j was performed by Eqs. (7), (8), and (12) for the (3+1) model of four indium atoms radial distribution around the absorbing As (named as a true model in this study), using $\sigma^2 = 0.005 \text{ \AA}^2$ and the value ε_j , given by the random generator routine²⁸ with the fixed noise amplitude ε_{max} (i.e., $|\varepsilon_j| \leq \varepsilon_{\text{max}}$). According to the results of²⁶ the uniform distribution of errors ε_j around the true value was used. The study of the statistical noise effect was performed for the amplitude values $\varepsilon_{\text{max}} = 0.1\%$, 0.5% , 1% , 2% , \dots , 10% , via the following scheme: (1) for each value of the noise amplitude ε_{max} , the 500 functions $\chi_m^{\text{st.n.}}(k_j)$ were calculated ($m = 1, 2, \dots, 500$), which differ one from another by the realizations of array $\{\varepsilon_j\}$; (2) each func-

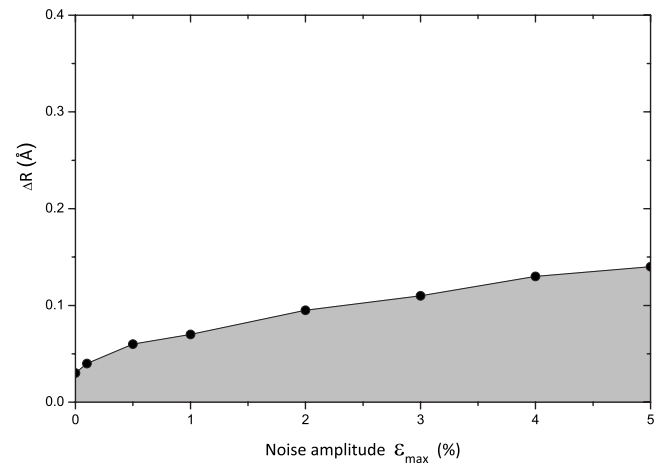


FIG. 5. Boundary values of ΔR in the true (3+1) model of As coordination by four In atoms, at which this model becomes preferable among others in FT analysis over $\Delta k = 3 \text{ \AA}^{-1}$, as a function of noise amplitude ε_{max} .

TABLE II. Results of FT over $\Delta k=3 \text{ \AA}^{-1}$ of $\chi^{\text{st.n.}}(k)$ for distorted coordination of As by four In atoms and of the fit by the true (3+1) model at different values of statistical noise ε_{max} . The structural parameters determined by the fit are compared with their values used in the direct calculations of $\chi^{\text{st.n.}}(k)$.

Noise amplitude, ε_{max}	Parameters R_1, R_2 (\AA), σ^2 (\AA^2) of analyzed $\chi^{\text{st.n.}}_m(k)$, used for its direct calculation at $N_1=3, N_2=1$	Values of parameters obtained by FT of $\chi^{\text{st.n.}}_m(k)$ ($m=1, \dots, 500$) on $\Delta k = 3 \text{ \AA}^{-1}$, by fitting of $F_m(R)$ and averaging over these 500 signals	
		(3+1) fitting model	Histograms of R_1 and R_2 distribution
0.1 %	$R_1 = 2.00$ $R_2 = 2.05$ $\sigma^2 = 0.005$	Model is preferable among others and gives: $\chi^2_v = 0.3$ $R_1 = 2.000 \pm 0.002$ $R_2 = 2.052 \pm 0.004$ $\sigma^2 = 0.005 \pm 0.001$	
0.1 %	$R_1 = 2.00$ $R_2 = 2.03$ $\sigma^2 = 0.005$	Model is not preferable. Its parameters: $\chi^2_v = 0.4$ $R_1 = 2.001 \pm 0.005$ $R_2 = 2.020 \pm 0.01$ $\sigma^2 = 0.0049 \pm 0.0001$	
1 %	$R_1 = 2.00$ $R_2 = 2.10$ $\sigma^2 = 0.005$	Model is preferable among others and gives: $\chi^2_v = 4.0$ $R_1 = 2.002 \pm 0.005$ $R_2 = 2.090 \pm 0.015$ $\sigma^2 = 0.005 \pm 0.001$	
1 %	$R_1 = 2.00$ $R_2 = 2.05$ $\sigma^2 = 0.005$	Model is not preferable. Its parameters: $\chi^2_v = 5.0$ $R_1 = 2.002 \pm 0.014$ $R_2 = 2.045 \pm 0.042$ $\sigma^2 = 0.005 \pm 0.001$	

tion $\chi_m^{\text{st.n.}}(k_j)$ was considered then as the unknown signal with parameters to be determined. This determination was performed applying FT to $\chi_m^{\text{st.n.}}(k_j)$ and the obtained $F_m(R)$ was fitted both by the single shell models (with varied parameters N , R , and σ^2) and by the alternative models for local structure distortions in the absorbing atom's coordination (varied parameters were σ^2 and R_i , $i=1,2,\dots$ —depending on the analyzed alternative model of atoms radial distribution); (3) under each value of noise amplitude ε_{max} , the obtained structural parameters of $\chi_m^{\text{st.n.}}(k_j)$, including the fit quality χ_p^2 , were averaged over all these 500 signals and histograms of R_i distribution were plotted.

Figure 5 shows the effect of the statistical noise on the boundary value of $\Delta R = |R_2 - R_1|$ —the difference of two interatomic distances in the true (3+1) model of local structure distortions, at which this model becomes preferable among others (single shell model, (2+2), (1+2+1) models, etc.) in the used FT analysis over $\Delta k = 3 \text{ \AA}$.

The more detailed information of the distinguishability of the true (3+1) model with different values of ΔR , at the values of statistical noise amplitude $\varepsilon_{\text{max}} = 0.1\%$ and 1% , is presented in Table II together with the determined values of structural parameters of (3+1) model and the histograms of R_1 and R_2 distribution.

The obtained significant reduction in the low bound ΔR in the problem of interatomic distances resolution by energy restricted x-ray absorption spectra, compared to that estimated by Eqs. (4) and (5), can be explained by the following most plausible reasons: (i) as was mentioned above, the expressions (4) and (5) are rough enough for XAS analysis since the boundary conditions for the signals, used to derive Eqs. (4) and (5), are weakly suitable for XAS; (ii) the use of the functional form for the fitting function, the same as of the studied signal, is equivalent (for the fit under the fixed signal's extension Δk and fixed R_{max}) to the increase in the sampling points number of the signal. Under this oversampling, the application of the nonlinear curve fitting procedure permits to analyze the asymmetry of the coordinating atoms Fourier peak in $F(R)$, defined now by the smaller steps δR , which results in the decrease in the low bound ΔR in the true

model of local structure distortions, when this model can be distinguished among others by the used approach.

IV. SUMMARY AND CONCLUSIONS

The analysis of applicability of the existed criteria for close distances resolution within XAS approach, based on FT and fitting procedures, is performed without losing generality by theoretical signals of different k dependencies. The following conclusions can be made: (1) The expression $\Delta R = \pi/(2 \cdot \Delta k)$, used in x-ray absorption spectroscopy to estimate the possibility of close interatomic distances resolution (Δk is the extension of the signal in the photoelectron wave numbers k scale), establishes the lower boundary for the difference $\Delta R = |R_2 - R_1|$ in the two parameters R_1 and R_2 of the arbitrary shape signal, which can be distinguished by FT and fit of $F(R)$ in general case—when the functional form of k dependence of the used fitting function differ from that of the studied signal. (2) If the functional form of k dependence of the fitting function is the same as of the studied signal $\chi(k)$ (as occurs in x-ray absorption spectroscopy) then the FT of $\chi(k)$ over $\Delta k = 3$ or 4 \AA^{-1} and the fit of $F(R)$, performed by alternative models of radial distribution of atoms around the absorbing one, enable to distinguish the true model among others beginning from $\Delta R = 0.03 \text{ \AA}$, and obtain the correct values of this model's parameters R_i and σ^2 . The revealed boundary value for ΔR is approximately ten times smaller than that estimated by expression (4). (3) Statistical noise in intensity of spectrum increases, according to the obtained dependence of Fig. 5, the boundary value of ΔR in the true model of local-structure distortions, at which it can be distinguished among other models by the used approach. Thus, the noise value of $\sim 1\%$, big enough for current XAS measurements, increases the boundary value of ΔR from 0.03 to 0.06 \AA .

ACKNOWLEDGMENTS

The authors are thankful to Vedrinskii R.V. and Kozinkin A.V. for helpful discussions.

- ¹J. A. van Bokhoven, A. M. J. van der Eerden, and R. Prins, *J. Am. Chem. Soc.* **126**, 4506 (2004).
- ²A. Szizybalski, F. Girgsdies, A. Rabis, Y. Wang, M. Niederberger, and T. Ressler, *J. Catal.* **233**, 297 (2005).
- ³S. Pascarelli, G. Aquilanti, W. A. Crichton, T. Le Bihan, M. Mezouar, S. De Panfilis, J. P. Itie, and A. Polian, *Europhys. Lett.* **61**, 554 (2003).
- ⁴M. Benfato, S. Della Longa, and P. D'Angelo, *Phys. Scr.* **115**, 28 (2005).
- ⁵M. Taillefumier, D. Cabaret, A.-M. Flank, and F. Mauri, *Phys. Rev. B* **66**, 195107 (2002).
- ⁶A. Filipponi, A. DiCiccio, and C. R. Natoli, *Phys. Rev. B* **52**, 15122 (1995).
- ⁷G. Smolentsev, A. V. Soldatov, and M. C. Feiters, *Phys. Rev. B* **75**, 144106 (2007).

- ⁸L. A. Bugaev, A. P. Sokolenko, H. V. Dmitrienko, and A. M. Flank, *Phys. Rev. B* **65**, 024105 (2001).
- ⁹L. A. Bugaev, J. A. van Bokhoven, A. P. Sokolenko, Ya. V. Latokha, and L. A. Avakyan, *J. Phys. Chem. B* **24**, 10771 (2005).
- ¹⁰L. A. Bugaev, F. Farges, E. B. Rusakova, A. P. Sokolenko, Ya. V. Latokha, and L. A. Avakyan, *Phys. Scr.* **115**, 215 (2005).
- ¹¹P. J. Riggs-Gelasco, T. L. Stemmler, and J. E. Penner-Hahn, *Coord. Chem. Rev.* **144**, 245 (1995).
- ¹²L. Brillouin, *Science and Information Theory* (Academic Press, New York, 1962).
- ¹³A. V. Oppenheim, R. W. Schaffer, and J. R. Buck, *Discrete-Time Signal Processing* (Prentice Hall, Englewood Cliffs, NJ, 1999).
- ¹⁴M. Newville Ph.D. thesis, University of Washington, 1995.
- ¹⁵D. C. Koningsberger and R. Prins, *X-ray Absorption: Principles*,

- Applications, Techniques of EXAFS, SEXAFS and XANES* (Wiley, N.Y., 1988).
- ¹⁶A. Filipponi and A. Di Cicco, *Phys. Rev. B* **52**, 15135 (1995).
- ¹⁷E. D. Crozier, J. J. Rehr, and R. Ingalls, *X-ray Absorption: Principles, Applications, Techniques of EXAFS, SEXAFS and XANES* (Wiley, N.Y., 1988).
- ¹⁸M. Newville, IFEFFIT web page and online documentation <http://cars9.uchicago.edu/ifeffit>
- ¹⁹A. L. Ankudinov, B. Ravel, J. J. Rehr, and S. D. Conradson, *Phys. Rev. B* **58**, 7565 (1998).
- ²⁰S. I. Zabinsky, J. J. Rehr, A. Ankudinov, R. C. Albers, and M. J. Eller, *Phys. Rev. B* **52**, 2995 (1995).
- ²¹L. A. Bugaev, Ph. Ildefonse, A.-M. Flank, A. P. Sokolenko, and H. V. Dmitrienko, *J. Phys.: Condens. Matter* **10**, 5463 (1998).
- ²²M. Newville, B. Ravel, D. Haskel, J. J. Rehr, E. A. Stern, and Y. Yacoby, *Physica B* **208&209**, 154 (1995).
- ²³G. Aquilanti and S. Pascarelli, *J. Phys.: Condens. Matter* **17**, 1811 (2005).
- ²⁴L. A. Bugaev, Ya. V. Latokha, L. A. Avakyan, G. Aquilanti, and S. Pascarelli, *AIP Conf. Proc.* **882**, 395 (2007).
- ²⁵A. V. Poiarkova and J. J. Rehr, *Phys. Rev. B* **59**, 948 (1999).
- ²⁶L. Incoccia and S. Mobilo, *Nuovo Cimento D* **3**, 867 (1984).
- ²⁷A. Filliponi, *J. Phys.: Condens. Matter* **7**, 9343 (1995).
- ²⁸D. E. Knuth, *The Art of Computer Programming*, Seminumerical Algorithms Vol. 2 (Addison-Wesley, Reading, MA, 1997).